AD-A160 310   CORRELATION AND COLLECTIVE MODES IN NARROW BAND   1/1
              MATERIALS(U) GEORGIA INST OF TECH ATLANTA SCHOOL OF
              PHYSICS M W RIBARSKY 02 MAY 85 AFOSR-TR-85-0879
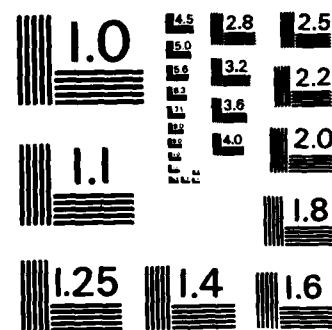UNCLASSIFIED AFOSR-80-0023   F/G 20/3   NL

END

MICROCOPY RESOLUTION TEST CHART

NATIONAL BUREAU OF STANDARDS-1963-A

REPORT DOCUMENTATION PAGE		READ INSTRUCTIONS BEFORE COMPLETING FORM
1. REPORT NUMBER A(?) 9	2. GOVT ACCESSION NO.	3. RECIPIENT'S CATALOG NUMBER
4. TITLE (and Subtitle) "Correlation and Collective Modes in Narrow Band Materials"		5. TYPE OF REPORT & PERIOD COVERED ~~Interim 1984~~ Final Oct. 1, 1984 to Sept. 30, 1985
		6. PERFORMING ORG. REPORT NUMBER
AUTHOR(s) Martin W. Ribarsky		8. CONTRACT OR GRANT NUMBER(s) AFOSR-80-0023
PERFORMING ORGANIZATION NAME AND ADDRESS Georgia Institute of Technology School of Physics Atlanta, Georgia 30332		10. PROGRAM ELEMENT PROJECT, TASK AREA & WORK UNIT NUMBERS 61102F 2301/A6
CONTROLLING OFFICE NAME AND ADDRESS Air Force Office of Scientific Research /NP Bolling AFB, Building 410 Washington, D. C. 20332		12. REPORT DATE May 2, 1985
		13. NUMBER OF PAGES
MONITORING AGENCY NAME & ADDRESS(if different from Controlling Office)		15. SECURITY CLASS. (of this report)
		15a. DECLASSIFICATION/DOWNGRADING SCHEDULE

16. DISTRIBUTION STATEMENT (of this Report)

Approved for public release;
Distribution unlimited.

17. DISTRIBUTION STATEMENT (of the abstract entered in Block 20, if different from Report)

18. SUPPLEMENTARY NOTES

19. KEY WORDS (Continue on reverse side if necessary and identify by block number)
Transition metals, copper, correlation, excitons, dielectric response, interband excitation, optical spectra, energy loss spectra, superconductivity.

20. ABSTRACT (Continue on reverse side if necessary and identify by block number)

Correlation and collective modes have been studied for systems with quite localized valence or conduction bands. In particular this research has been concerned with localized electron-hole states and how they contribute with other excitations to the dynamical response of the system. Important aspects studied have been the effects of exciton or exciton-like states on super-conducting properties, electron energy loss spectra and optical spectra. Initially the system studied has been CuCl for which a tight-binding model

DD FORM 1473 EDITION OF 1 NOV 65 IS OBSOLETE
1 JAN 73

was used. The results show that strong effects due to localized excitations of d-band electrons greatly affect the dynamical response and the effective electron interaction. Off-diagonal matrix elements of the inverse dielectric matrix are important, and the exchange interaction greatly affects the excitation spectrum, producing exciton resonances in the band gap. The exciton resonance in the dynamical response is necessary to obtain the appropriate attractive effective electron interaction for superconductivity. Models have also been set up to relate the dynamical response including local field effects to the superconducting transition temperature and gap function. The strong localization effects also will affect the loss spectra and optical spectra.

Accession For

NTIS GRA&I	X
DTIC TAB	☐
Unannounced	☐
Justification	

By

Distribution/

Availability Codes

| Dist | Avail and/or Special |

A-1

DTIC COPY INSPECTED

Table of Contents

85 1 0 11 12

I. Research Objectives

The overall objective of this work is to study correlation and collective modes for systems with quite localized valence or conduction bands. For these systems one must consider the effects of localized excitations and collective modes to understand large scale correlated states such as superconductivity or the interaction of the system with optical or electronic probes. In certain cases, such as for narrow-band insulators, one must consider these effects to understand even ground state properties. In particular this research has been concerned with localized electron-hole states and excitonic modes and how they contribute with other excitations to the dynamical response of the system.

The effect of strongly localized excitations on the superconducting properties of a material can be significant. We are most concerned with the effect on the superconducting mechanism itself. For systems such as oxidized Cu or CuCl, there are some experimental indications that the usual phonon-coupling mechanism is augmented or even dominated by an exciton-coupling mechanism. We have developed some models to describe the excitation structure in terms of excitons alone and with these have studied local field effects on the dynamical response. Our objective is to discover whether excitons can cause an attractive response.

The effects of localized excitations on the response to optical or electronic probes is known to be significant. Our exciton models have already successfully explained the optical absorption due to intrinsic excitons in several materials. Our objective here is to provide a detailed description of the effects of local field corrections and umklapp scattering terms on the dielectric response of these materials. The calculations described in this report show that the local field corrections are important in general for tightly-bound systems and in particular for impurity-doped CuCl under pressure. Also,

the calculations reveal a rich exciton resonance structure which is quite sensitive to the strength of the electron exchange interaction, and which provides possibly new and important details about the nature of the excitonic states in narrow band systems.

Our models are leading to a clearer picture of the superconducting state in narrow band materials and of the conditions which ensure optimized properties. Also we are obtaining a better understanding of the electronic excitation structure of these systems and of the structure of the optical absorption and electron energy loss spectra. In addition we are developing methods for describing the effect of correlations between metal and adsorbate valence electrons on the bonding and vibrational excitations of metal-adsorbate systems. We will discuss these calculations further below.

II.   Investigations of Electronic Structure in Narrow Band Materials

We have developed several theoretical methods and models for dealing with
the electronic structure and properties of narrow band materials. Among these
are:

1.   Tight-binding models - These are models which describe the d- and s-
valence band electronic structure of materials. They can be used to give the
density of states of transition metals, alloys and compounds.

2.   Surface and grain boundary segregation models - Using the tight-binding
density of states and minimizing the system free energy, one can obtain the surface
and grain boundary composition. We have extended this model to the surface segre-
gation of ternary alloys and are extending it to include d-band effects in
grain boundary segregation. We have also developed a model for the diffusion
of a non-uniform implant profile in the presence of a surface. The model shows
that considerable nonequilibrium implant surface segregation can occur under
certain conditions even if there is no equilibrium surface segregation.

3.   Excitonic Superconductivity Models - We have used the tight-binding
model to develop a model for excitonic effects on the attractive effective
electron-electron coupling which includes local field effects and the effects
of valence and conduction band structure. We have also developed a model for
the superconducting transition temperature and gap equation which includes
local field and excitonic effects.

4.   Cluster calculation methods - We have extensive experience with
ab-initio Hartree-Fock and linear-combination-of-atomic orbitals Xα (LCAOXα)
molecular cluster methods. These methods give a detailed description of local
electronic structure and they are self-consistent so that they describe the
rearrangement of the electrons even for changes in complicated geometries. In
particular the methods are useful for defects in the bulk or at surfaces or

3

boundaries, for studying certain localized catalytic and adsorption processes, and for systems of complicated local geometries which are likely to have localized electronic states. We have extended the methods to long range systems by applying embedding models which include the dominant effects of the environment on the cluster. Our recent calculations are for H_2O adsorbed on Cu surfaces where we explore the correlation of Cu d and s electrons with O p and s electrons to produce surface-adsorbate bonds. Our calculations give the first detailed agreement between theory and experiment for H_2O monomers on a Cu surface and provide a complete description of the bonding mechanism for this important system. Some of our papers and presentations in the past two years in the general area of properties of transitions metals or narrow band materials are:

"Exciton Coupling and the Effective Electron Interaction in Narrow Band Materials," A. P. S. March Meeting, Los Angeles (1983).

"Local Field Effects on Exciton Coupling in CuCl and CdS Under Pressure," High Pressure in Science and Technology (Elsevier, New York, 1984).

"Local Field Effects Due to Excitons and the Superconducting Coupling Constant," A. P. S. March Meeting, Detroit (1984).

"The Diffusion of Implanted Ions near Surfaces and Grain Boundaries," A. P. S. March Meeting, Detroit (1984).

"Electronic Structure Calculations of Water on a Copper Surface," 44th Physical Electronics Conference (June, 1984).

"Molecular Orbital SCF Cluster Model of H_2O Adsorption on Copper," A. P. S. March Meeting, Baltimore (1985).

"Effects of Local Fields on the Superconducting Mechanism," A. P. S. March Meeting, Baltimore (1985).

"A Molecular Orbital SCF Cluster Model of H_2O Adsorption on Copper," submitted to Rapid Communications, Phys. Rev. B.

"Exciton Mechanism of Superconductivity in CuCl," to be submitted.

III. Local Field and Exchange Effects in the Dielectric Response

A. Tight Binding Calculations of the Electronic Response

Our tight binding model is based on a model developed by Prakash and Joshi[1] and extended by Hanke to the lattice dynamics of Pd and Ni.[2] One assumes that the band structure of the system is adequately described by a non-interacting band model. Then one connects the high-symmetry points in the band structure according to compatibility and which atomic level they represent by symmetry (for example Γ_{12} connects with L_3 in FCC structures because both states represent $d_{m=2}$). The bands are then described as parabolas with an effective mass assigned to give them the optimal shape. The Bloch states in the tight-binding formulation are just

$$\Psi_\nu^{\vec{k}}(\vec{r}) = \frac{1}{N^{1/2}} \sum_\ell e^{i\vec{k}\cdot\vec{R}_\ell} u_\nu(\vec{r}-\vec{R}_\ell) \ ,$$

where u_ν is the appropriate atomic wave function. Although these approximations are fairly extreme, the model dielectric screening, when used in calculations of the phonon dispersion for Pd and Ni, gives good results.[2]

The simplest band model for the metallic systems of interest here is an s-d band model. We can augment this model by assuming the d bands are hybridized with, for example O or Cl p states in the case of the oxide or chloride of Cu. In the s-d band model, the dielectric matrix is

$$\underline{\varepsilon} = \underline{1} - \underline{\varepsilon}_{ss} - \underline{\varepsilon}_{sd} - \underline{\varepsilon}_{ds} - \underline{\varepsilon}_{dd} \ . \tag{1}$$

When d-d intraband terms contribute, our calculations[3] indicate that $\underline{\varepsilon}_{dd}$ dominates in Eq. (1). Hanke also found this to be the case for Pd and Ni.[2] However, for calculations of the superconductivity properties where the exciton positions and strengths are important, one cannot neglect the s-d interband terms since they contribute to the exciton structure. To simplify the present

5

discussion, we will focus on only the d-d intraband and interband terms. One can easily include the s-s terms at any stage in the calculation by replacing V by V/ε_{ss}.[2] Focusing on the d-d terms, we use a zero overlap approximation where we neglect intersite overlap. The Coulomb and exchange interaction matrices take the simple form

$$V_{m\ell,m'\ell'}(q) = \sum_G A^*_{m\ell}(\vec{q}+\vec{G})\ V(\vec{q}+\vec{G})\ A_{m'\ell'}(\vec{q}+\vec{G}) \tag{2}$$

$$V^x_{m\ell,m'\ell'}(q) = \sum_G A^*_{m\ell}(G)\ V_{\vec{G}}\ A_{m'\ell'}(G)$$

where

$$m,m'\ :\ \text{unoccupied d states}$$

$$\ell,\ell'\ :\ \text{occupied d states}$$

and

$$V_{\vec{q}} = \frac{4\Pi e^2}{q^2}$$

The overlap matrix $A_{m\ell}$ is

$$A_{m\ell}(\vec{q}+\vec{G}) = \int u^*_m(\vec{r})\ e^{i(\vec{q}+\vec{G})\cdot\vec{r}}\ u_\ell(\vec{r})d\vec{r}\ .$$

The zero-overlap approximation in Eq. (2) allows us to include exchange effects just as easily as Coulomb effects, which is not the case when overlaps are included.[4]

It is most convenient to use the notation of Hanke and Sham to construct $\underline{\varepsilon}^{-1}$.[4] However in the present tight-binding case, the matrix elements are over the band states themselves rather than just the local orbital basis. Then

$$\underline{\varepsilon}^{-1}(\vec{p},\vec{q};\omega) = \sum_{\vec{R}_a, \vec{R}_b} e^{i\vec{p}\cdot(\vec{R}_a-\vec{R}_b)} \left[\delta_{\vec{R}_a,\vec{R}_b} - \underline{S}(q,\omega;\vec{R}_a,\vec{R}_b) \right] \tag{3}$$

where

$$\underline{S} = \underline{N}^{O}[\underline{1} - (\underline{V} - \frac{1}{2}\underline{V}^{X})\ \underline{N}^{O}]^{-1}\ ,$$

and the non-interacting polarizability $\underline{N}^{O}$ is given in Eq. (2.10) of Ref. 4 with all expansion coefficients C set equal to one.

It is apparent from Eqs. (1-3) that we have a frequency- and momentum-dependent formulation of the dielectric matrix including exchange which is in terms of few important parameters. The Coulomb and exchange interactions in Eq. (2) are comprised of only three and four elements, respectively, for the case of d-d interband and intraband transitions in CuCl. The magnitude of each element depends on the extent of the atomic-like wave function on Cu. The widths and frequency positions of structures in $\underline{N}^{O}$ depend directly on the energy band widths and positions. The positions and dispersions of excitons and plasmons in $\underline{\varepsilon}^{-1}$ will then depend on combinations of these quantities. Thus by evaluating the dependence of the dielectric response and exciton and plasmon structures on these parameters and then tabulating the values of these parameters for many materials, we may know the trends in correlation and collective phenomena for a wide range of narrow band systems. We present some results from such an evaluation in Sec. IV.

B. Dielectric Response Model of Superconductivity Including Local Field and Exchange Effects

The purpose of this section is to describe a model for a superconducting state in terms of Coulomb interactions alone. Thus the dielectric response of the surrounding medium must be included explicitly to obtain an attractive interaction between electrons. The dielectric response is frequency dependent and contains exchange interactions so that one may evaluate the strength of both the exciton and plasmon pairing mechanisms.

7

We have developed a method in terms of Bloch states which includes the effects of the dynamical dielectric response on the superconducting properties.[5] The method follows the development of Takada,[6] except that it is generalized to a Bloch basis set to take into account local field effects. Our expression for the critical temperature T_c is

$$T_c = 1.134 \ \varepsilon_F \ \exp \left[\frac{1}{\beta_{no}} + \int_{-1}^{\infty} \frac{dx}{2|x|} \sum_{n_3} \frac{\Delta_{n_3}(x)}{\Delta_n(o)} \right.$$

$$\left. K_{nn_3}(o,x)/\beta_{no} - \theta(1-|x|) \right] \quad , \tag{4}$$

$$x \equiv \omega/\varepsilon_F \ ,$$

where

$$\beta_{no} \equiv \sum_{n_3} \frac{\Delta_{n_3}(o)}{\Delta_n(o)} \ K_{n_3 n_3}(o,o) \ ;$$

n, n_3 refer to Bloch states; ε_F is the Fermi energy; and Δ_n is the gap function. The kernel K is a generalization of the usual homogeneous form (see Ref. 6) which contains the screened interaction

$$\underline{\varepsilon}^{-1}(\vec{p},\vec{q},\omega) \ \underline{V}(\vec{p},\vec{q})_s$$

where $\underline{V}$ is the Coulomb interaction matrix in the Bloch basis. This form of $\underline{\varepsilon}^{-1}$ is just the one we considered in the last section using the tight-binding model. In addition, we obtain an expression for $\phi_n(x) = \Delta_n(x)/\Delta_n(\phi)$:

$$\phi_n(x) = K_{n,n}(x,o)/K_{nn}(o,o) \tag{5}$$

$$- \int_{-1} \frac{dx'}{2|x'|} \sum_{n_3} \frac{\Delta_{n_3}(x')}{\Delta_n(o)} \left[K_{nn_3}(x,x') - \frac{K_{nn}(x,o)}{K_{nn}(o,o)} K_{nn_3}(o,x) \right]$$

8

We can treat Eq. (5) as a linear integral equation and solve for $\phi_n(x)$ and then find T_C using Eq. (4). Equations (4) and (5) are new results for inhomogeneous periodic systems which reduce to the previously found homogeneous equations.[6]

IV. Tight-Binding Calculations of the Dielectric Response for CuCl

Experimental measurements of anomalously large diamagnetism[7-9] in CuCl

samples under pressure from 5 to 15 kb and at temperatures up to 240° have

stirred considerable interest in the possibility of high temperature superconductivity.

Calculations of the valence and conduction bands[10-12] all indicate CuCl is a

direct gap semiconductor with a zincblende structure and that it remains so

under the pressures used in the experiments. However, Collins, et al.[13] have

proposed a mechanism for the anomalous diamagnetism based on the presence of

impurity levels such as 0^{--} just below the conduction band edge. They suggest

that under pressure the X point moves down and that the 0^{--} levels pressure-ionize

to produce free carriers around the X point. The lowering of the X point under

pressure to a position degenerate with the Γ point is supported by the calculations

of Kunz and Weidman.[10] Collins et al.[13] then show that an exciton-mediated high

temperature super-conducting state can exist assuming an appropriate exciton-

electron interaction and density of free carriers. Nobody, however, has addressed

the fundamental question of whether the exciton-mediated electron-electron interaction

is attractive. This is the purpose of the present calculations.

The equilibrium valence band structure for CuCl[11] is divided into three non-

overlapping regions as shown in Fig. 1. The lowest VB1 band is 90% Cl 3s character

and is between 10 and 12 eV from the predominantly (75%) Cl 3p VB2 band. In our

calculations we are only interested in the mostly Cu 3d VB3 band which is 3.5 eV

above VB2. The VB3 band has a lower, nearly dispersionless subband and a higher

subband 1.5 eV wide which contains 24% Cl 3p and 76% Cu 3d character at the zone

center. The magnitude of these orbital hybridizations agrees well with experimentally-

deduced values based on exciton spin-orbit splitting (25% Cl 3p)[14] and other

measurements. The lowest conduction band CB1 is mostly Cu 4s at the zone center

but has d-p character at $X_3(3)$. The calculations show that the valence bands

remain unchanged for moderate lattice contractions, but the conduction bands drop

at the BZ edge.[10-12] The insert in Fig. 1 shows the bands VB3 and CB1 in the calculation of Kunz and Weidman.[10] Here a 1% lattice contraction, consistent with the pressure used by Chu et al.[8] in their diamagnetism measurements, has rendered the points Γ_1 and X_3 nearly degenerate.

We have rendered the bands of Kunz and Weidman in the effective mass approximation so that the band energy is

$$E_{nk} = E_{on} + \frac{h^2 k^2}{2m_n}$$

where m_n is the effective mass and E_{on} is the energy at the bottom of the band. For the VB3 bands we have used the Γ and X points to determine the effective masses (see Prakash and Joshi for details)[1] and have ignored the non-degeneracy at X in the two subbands. For the conduction bands we have connected $\Gamma_{15}(3)$ to $X_3(3)$ and $\Gamma_1(\ )$ to $X_1(3)$ because these pairs are s-like and d-p like, respectively,[15] and we must connect points allowing the same symmetry when we assume non-hybridized bands.[1] The curvatures of the bands near $X_3(3)$ and $X_1(3)$ suggest an avoided crossing of this type. The zone boundary at X is at .615 a.u. for CuCl; but because we are using a spherical approximation for the energy bands, it is appropriate to use the Wigner-Seitz sphere radius to define the Fermi momentum. This value is .605 a.u. All the band structure parameters are given in Table I.

Since the upper valence band and the lowest conduction band at the X point have Cl 3p character as well as Cu 3d character, we must take hybridization into account. We can do this by allowing the conduction bands to be a Cu 3d-Cl 3p anti-bonding state. This hybridization is allowed because both Γ_{15} and X_3 can have d-p character. We use a mixing of 75% Cu and 25% Cl for the bonding state and 25% Cu and 75% Cl for the anti-bonding state. Besides being consistent with the experiment, this result is in agreement with calculations at Γ_{15}.[12] For the

atomic Cu 3d levels we choose the wavefunction obtained by Wachters,[16] and for the

Cl 3p levels we use the wavefunctions of Veillard.

In the calculations of the dielectric response reported here, we have used

the above model for CuCl under pressure. We have assumed a small concentration of

free carriers resides at the conduction band X point (degenerate with the Γ point

in this case), and we have neglected excitations from the valence bands to the

s-like conduction bands around Γ. Since d-d transitions dominate the dielectric

matrix[29] this is a good approximation for calculations where exciton structure

is not important. Such is the case for the optical absorption away from the

exciton peaks for this system, or for the dielectric response of the four-fold

coordinated compounds of Zn or Cd, which do not have s-like lowest conduction bands.

However, for calculations of superconducting properties, the dp-s transitions

should be included because the exciton structure is important. Nevertheless, even

for this case the following calculations give useful results.

We can study local field effects in our test system by looking at the matrix

elements of $\underline{\varepsilon}^{-1}(\vec{q},\omega)$ defined in Sec. IIIA. If local field effects were important, off-

diagonal matrix elements would be small. Therefore we compare in Fig. 2a the matrix elements

$\underline{\varepsilon}^{-1}_{V2C,V2C}$ and $\underline{\varepsilon}^{-1}_{V2C,CC}$ where V2C signifies transitions from the top valence

band to the conduction band and CC signifies intraband transitions from filled to

empty conduction band states. The momentum chosen for these calculations is $.103q_f$,

and the energy range, 0.05-0.20 a.u. (1.36 - 5.44 eV), is in the band gap of our

test system. Thus, $\underline{\varepsilon}^{-1}(\vec{q},\omega)$ is real, and there is no absorption except at the

exciton poles. Note that since we have ignored dp-s transitions, our system acts

as if it had an indirect gap. If we included the lowest s conduction band, the

band gap would only be .150 a.u. The results in Fig. 3a show that the off-diagonal

element $\varepsilon^{-1}_{V2C,CC}$ is indeed significant over the whole frequency range and that

local field effects cannot be ignored. To determine its dependence on lattice

vector, we plot $\varepsilon^{-1}_{V2C,V2C}$ (at $\vec{R}=\vec{R}'=0$) versus $\varepsilon^{-1}_{V2C,V2C;1,1}$ at the first

lattice vector ($\vec{R}=\vec{R}'=a/2(1,1,0)$) in Fig. 3b. Again we find $\varepsilon^{-1}_{V2C,V2C;1,1}$

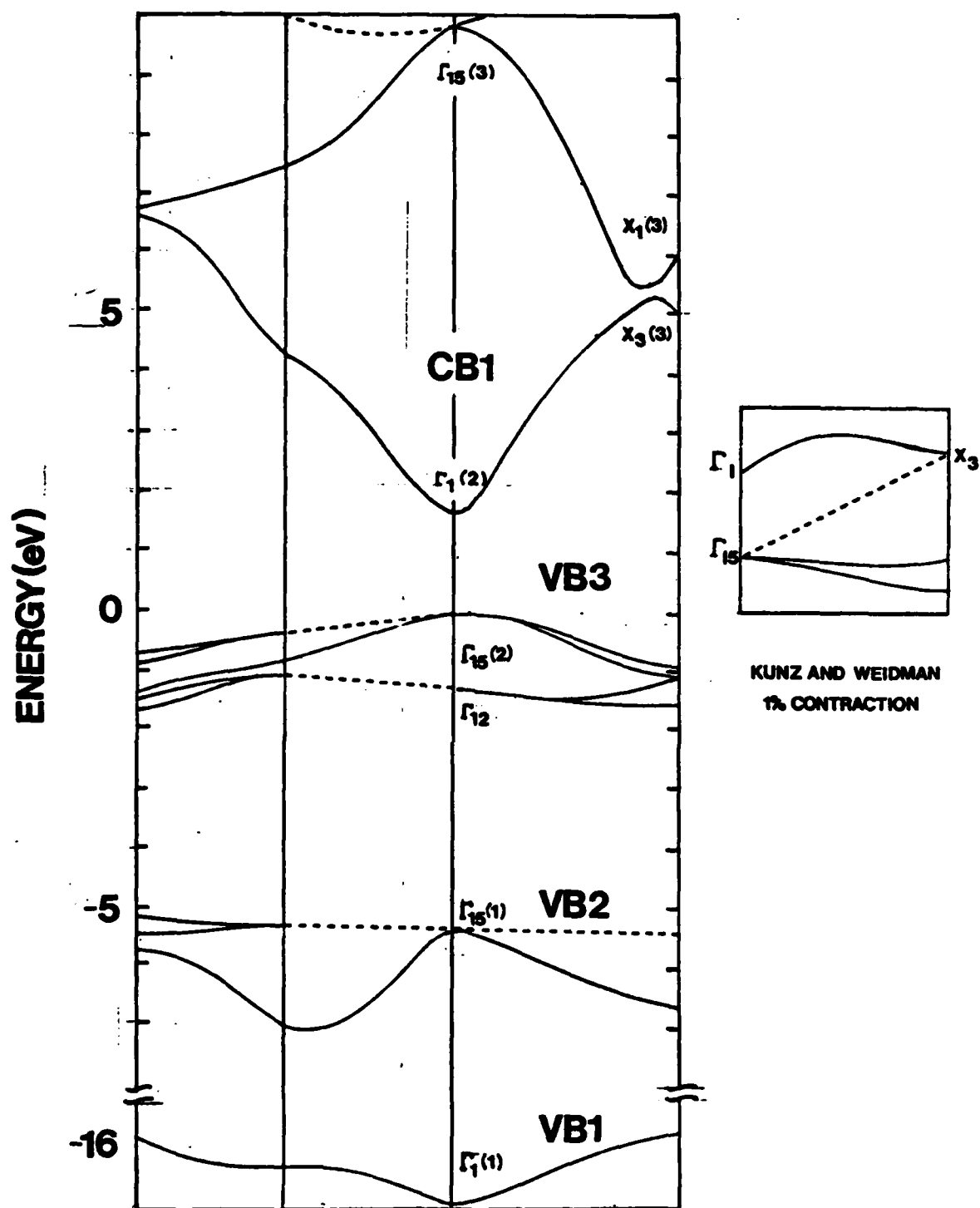**ENERGY(eV)**

CB1

$\Gamma_{15}(3)$

$X_1(3)$

$X_3(3)$

$\Gamma_1(2)$

VB3

$\Gamma_{15}(2)$

Γ_{12}

$\Gamma_{15}(1)$ VB2

VB1

$\Gamma_1(1)$

Γ_1

X_3

Γ_{15}

KUNZ AND WEIDMAN
1% CONTRACTION

Fig. 1 **EQUILIBRIUM ENERGY
BANDS OF CuCl**

13

TABLE I. Band structure parameters for CuCl under 1% contraction

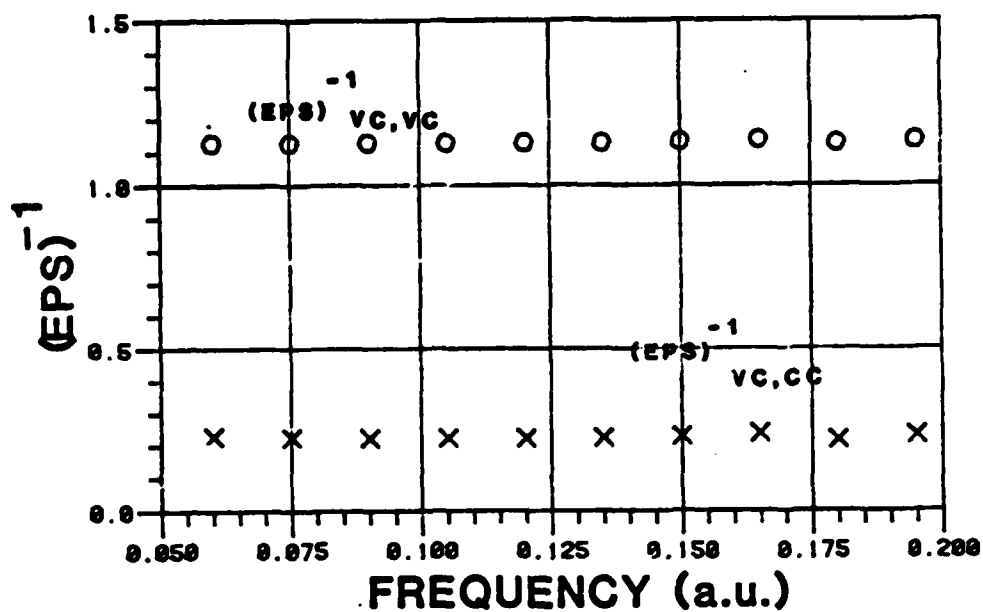| lattice parameter	10.215 a.u.	energy levels at high symmetry points	
crystal structure	zincblende	(a.u.)	
effective masses (in units of m_e):		Γ_{12}	−.250
$m\{\Gamma_{12} - (X_1, X_2)\}$	20	$\Gamma_{15}(2)$	−.105
$m\{\Gamma_{15}(2) - (X_3, X_5)\}$	−2.21	$\Gamma_1(2)$	.045
$m\{\Gamma_1(2) - X_1(3)\}$	1.28	$\Gamma_{15}(3)$	.220
$m\{\Gamma_{15}(3) - X_3(3)\}$	−1.05	$X_1(2), X_2$	−.241
		$X_5(2), X_3(2)$	−.188
		$X_3(3)$	.045
		$X_1(3)$	.188

Band Gap: .150 a.u. (4.08 ev)

14

Fig. 2a Comparison of the matrix elements $\varepsilon^{-1}_{V2C,V2C}$ and $\varepsilon^{-1}_{V2C,CC}$ at $q = .103\ q_f$.
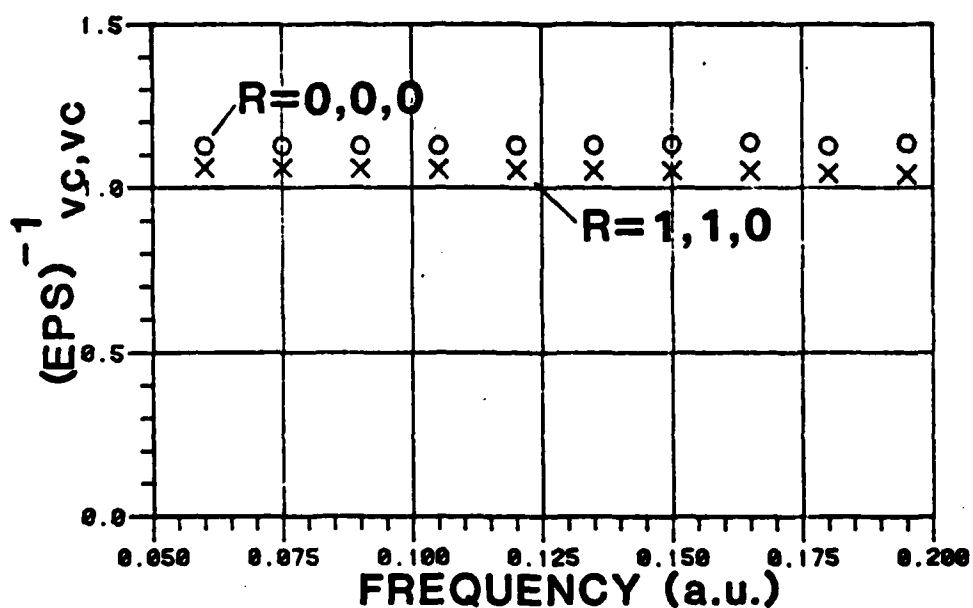

Fig. 2b Comparison of $\varepsilon^{-1}_{V2C,V2C}$ at $\vec{R} = (0,0,0)$ and $\vec{R} = a/2(1,1,0)$ for $q = .103\ q_f$.

15

to be significant so that we cannot neglect the dependence on lattice vector. In fact, we find it necessary to include through next nearest neighbor lattice vectors so that we have matrix elements for 19 vectors for the V2C,V2C transition. Our conclusions show that the recent model for the dielectric response of Fiorino and Del Sole,[17] which only includes terms for $\vec{R} = \vec{R}' = 0$ is greatly oversimplified.

The exciton pole structure is interesting to study because it illuminates the dynamical structure of $\underline{\varepsilon}^{-1}(\vec{q},\omega)$. True excitons exist only in the band gap, where there is no absorption. The true excitons are at the poles of $\underline{\varepsilon}^{-1}$ which are determined by the zeros of the factor

$$\left[\underline{1} - (\underline{V} - \tfrac{1}{2}\underline{V}^X) N^O \right]$$

in Eq. (3). We find the zeros by searching for the frequency at which the determinant Det of this factor is zero. In Fig. 3a we show the results for Real (Det) at $q = .103q_f$. As one can see, Real (Det) crosses zero only once in the band gap for this q, and thus there is only one exciton. The insert in Fig. 3a shows the region of the crossing in detail and can be used to determine the strength of the exciton since

$$\text{Det} \simeq f\ (\omega - \omega_{ex})$$

near the pole ω_{ex}, where f is the strength. We find the exciton to be quite strong so that it should produce a higher transition temperature in our model. We can see the effect on the screened interaction by looking at the matrix element $(\underline{\varepsilon}^{-1}\underline{V})_{CC,CC}$ in Fig. 3b. As we noted in Sec. IIIB, this matrix element determines the dynamics of the kernel K in the superconducting gap function. The matrix element goes dramatically negative, as it should, for frequencies greater than ω_{ex} indicating the attractive interaction which results in superconductivity.
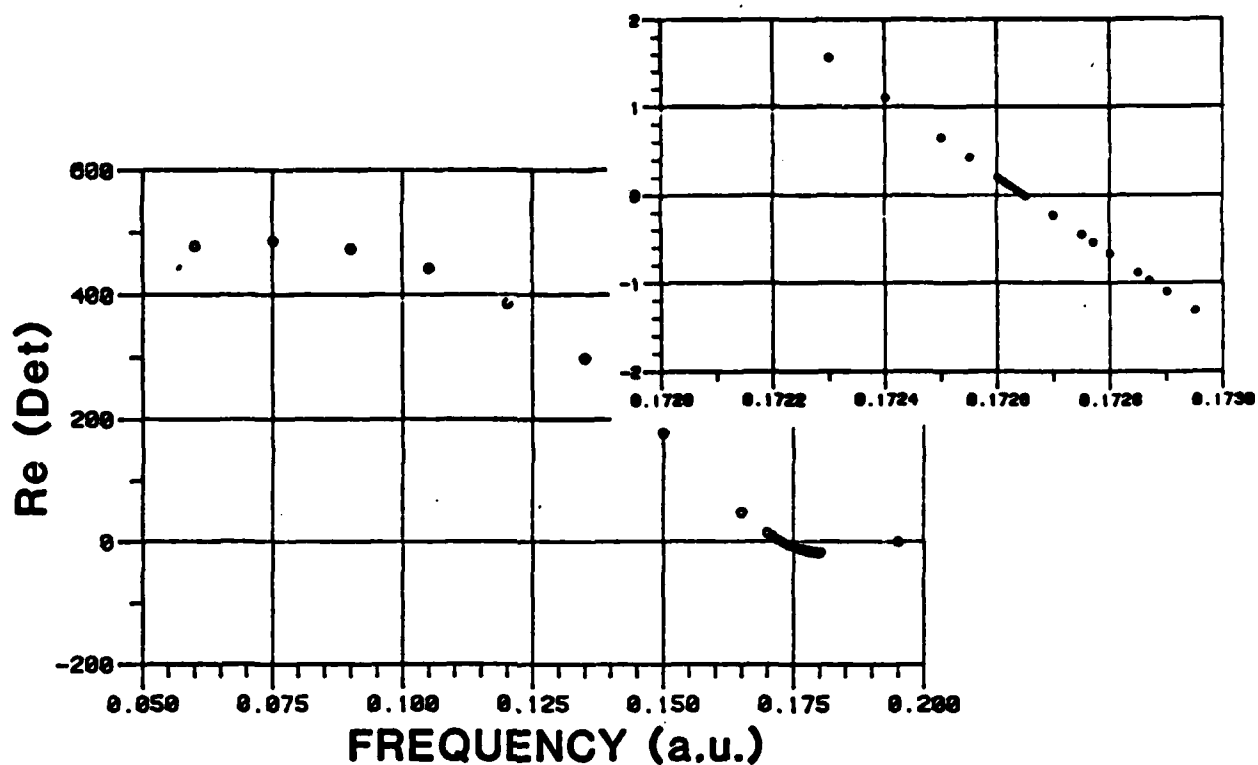
16

Fig. 3a Real part of the determinant of $\left[\underline{1}-(\underline{V}-\tfrac{1}{2}\underline{V}^{x})\underline{N}^{0} \right]$ at q= .103 q_f.
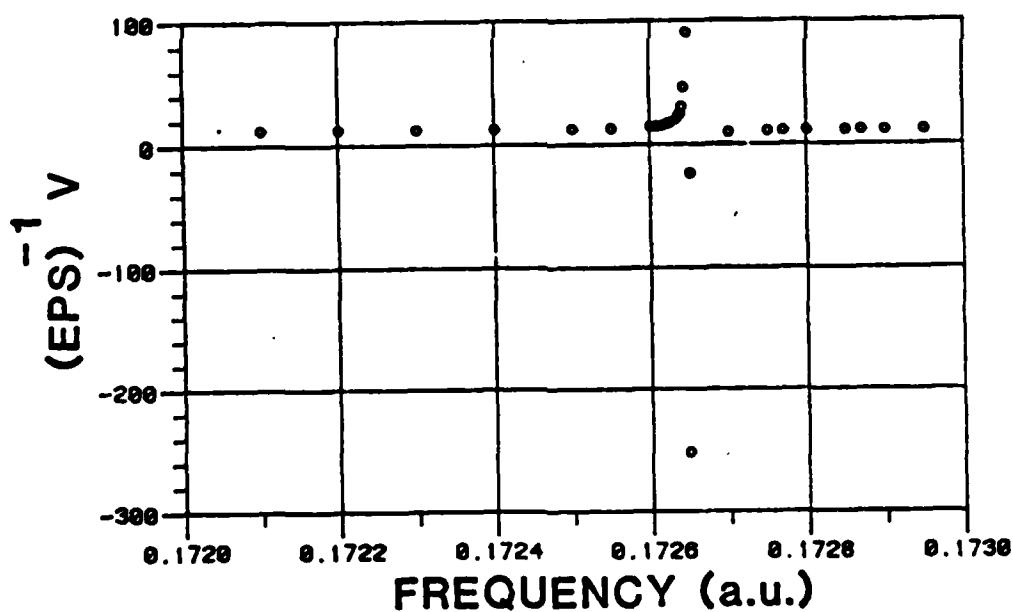

Fig. 3b Real part of $(\underline{\varepsilon}^{-1}\underline{V})_{CC,CC}$ at q= .103 q_f.

The frequency positions of excitons and exciton-like structures in the dielectric response are determined by the magnitude of the elements in $\underline{V}^x$. As these matrix elements diminish in magnitude, the exciton moves to higher frequency and eventually disappears. We can see this effect in Fig. 4 where we plot Real (Det) for $\underline{V}^x = 0$. The exciton pole has disappeared from the band gap. These results show that one can vary the magnitudes of the elements in $\underline{V}^x$ to match the experimental exciton energies and thus gain important information about the exchange interaction.

We may also study the dependence of the excitons on momentum q. We compare Real (Det) for $q = .103q_f$ with that for $q = .2q_f$ in Fig. 5. For excitations from our valence bands to the dp-like conduction bands, the gap diminishes for larger q values. Thus we see a crossing of zero at lower frequency for $q = .2q_f$, but we also see several other crossings as well. It may seem surprising that so many exciton poles appear in a system with only two valence bands and one conduction band and only a few distinct exchange matrix elements. But the maximum number of poles allowed is determined by the dimensionality of the $\underline{\epsilon}^{-1}$ matrix, and thus excitons can arise from elements with non-zero $\vec{R}$. For example, in our sytem there would be 19 possible exciton poles for each interband excitation. This is a fascinating aspect of the exciton pole structure which has not been studied before.

The effects of exciton-like transitions on the interband absorption part of the dielectric response also came out of our calculations, but we do not present those results here. We are now adding the more complicated dp to s excitation terms to our dielectric response formalism, and when that is done we will have a complete formulation for CuCl.
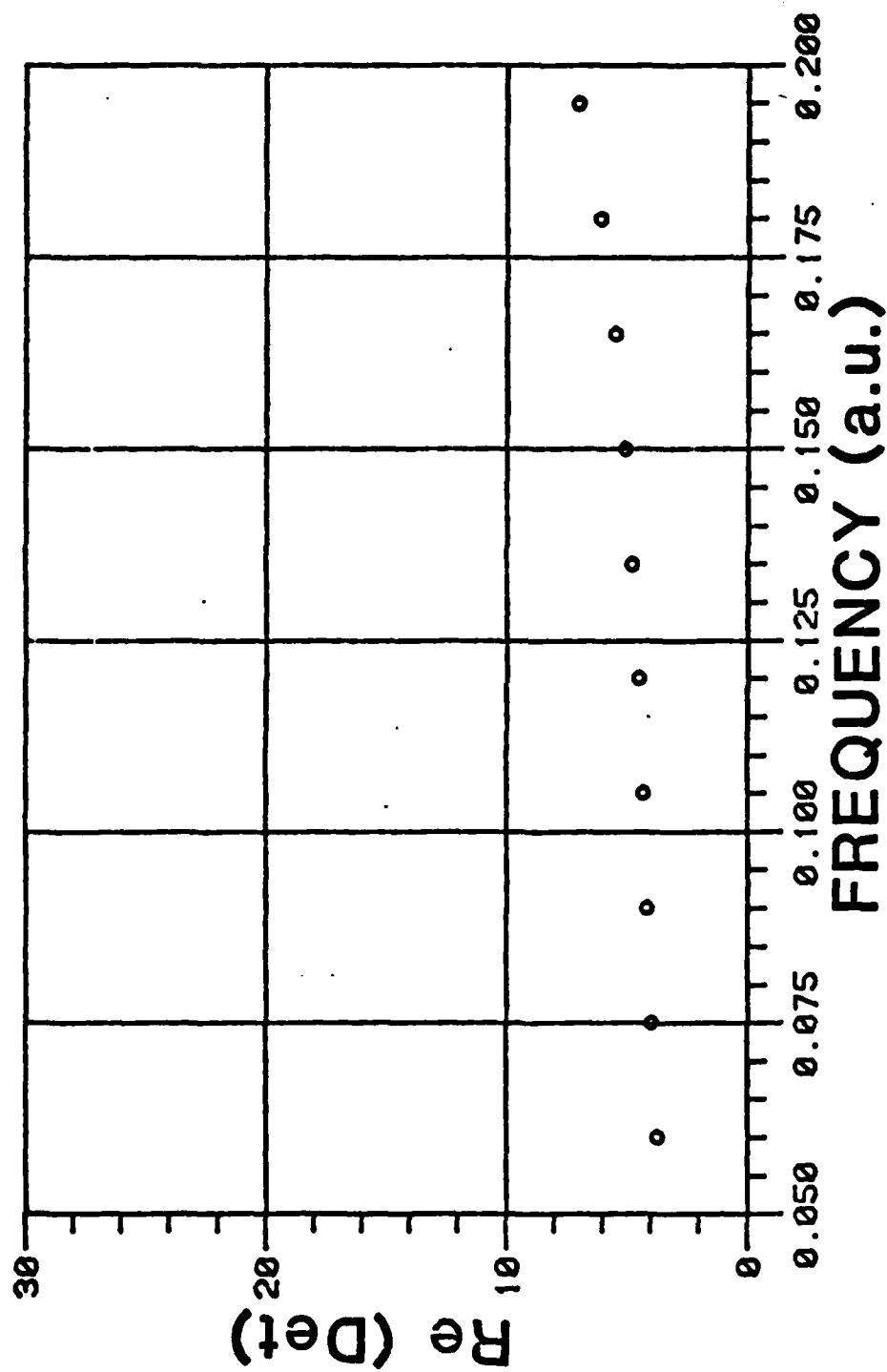
FREQUENCY (a.u.)

Re (Det)

30

20

10

0

0.050 0.075 0.100 0.125 0.150 0.175 0.200

Fig. 4 Real part of determinant defined in Fig. 4a for $\underline{V}^x=0.0$ at $q=.103\ q_f$.
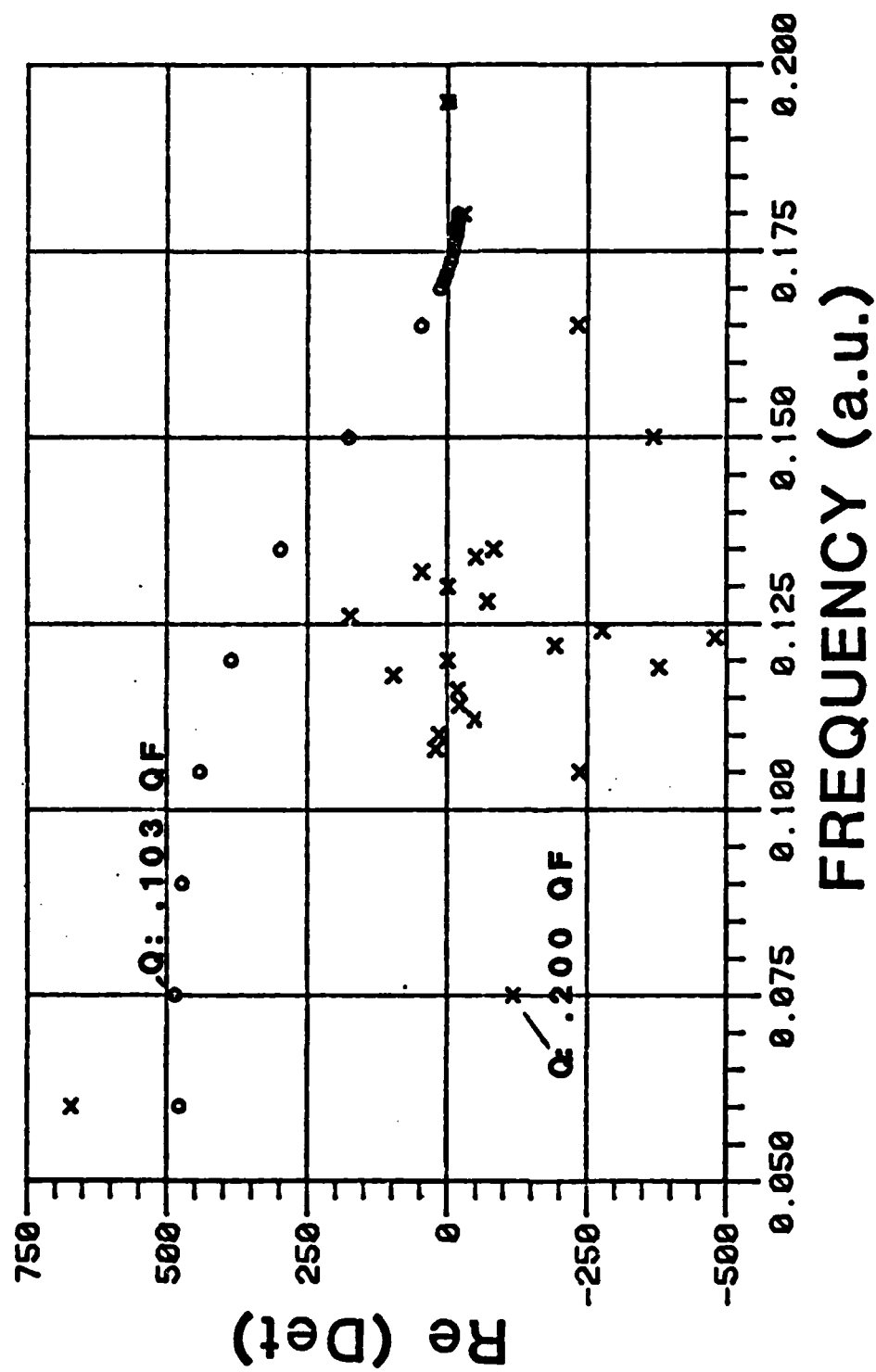
19

Fig. 5 Real part of determinant defined in Fig. 4a at q= .103 q_f and q= .200 q_f.

V. Localized Bonding States for Water Adsorbed on Copper

We have recently used another approach to describe the local electronic con-
figurations and the correlation which comes about via bonding in adsorbate-metal
surface systems. We have used linear combination of atomic orbitals X_α[18] (LCAO X_α)
cluster calculations to study H_2O monomers on a Cu surface. Recently experimenta-
lists have isolated these monomers on a metal surface for the first time and studied
them with high resolution EELS.[19] Understanding the nature of the bonding for this
system is important due to the physical and chemical processes involving H_2O that are
of fundamental and technological interest such as corrosion, certain catalytic re-
actions and electrochemical processes in acqueous solution. We have elucidated the
bonding mechanism for this system,[20] and our results can be generalized to other
H_2O-metal surface systems.

Our calculations for small clusters arranged to simulate H_2O adsorbed on a Cu
(100) surface give results for the binding energy, basic bonding mechanism and
orientation of H_2O monomers [18, 20] in good agreement with results which can be
inferred from the experimental data.[19] The calculations show that the H_2O is
adsorbed at the on-top site with the oxygen end down and a binding energy of .38 eV.
The molecular H_2O plane is tilted by an angle of 67° from the Cu-O axis. The amount
of tilt is related to the site chosen by the H_2O molecule, and thus the adsorbate
vibrational spectra can be used to determine the site preference on a metal surface.
The structural parameters for the H_2O within the cluster are close to those for the
free molecule. The bonding involves the H_2O lone pair orbitals and the top-most
valence and lowest conduction band states in the metal complex. Lastly an analysis
of the vibrational states for the cluster yields frequencies in generally good
agreement with the experimental vibrational frequencies.

21

VI. <u>References</u>

1. S. Prakash and S. K. Joshi, Phys. Rev. B <u>2</u>, 915 (1970).

2. W. Hanke, Phys. Rev. <u>B</u> 8, 4591 (1973).

3. M. W. Ribarsky, <u>High Pressure in Science and Technology</u> (Elsevier, New York, 1984).

4. W. Hanke and L. J. Sham, Phys. Rev. B <u>12</u>, 4501 (1975).

5. M. W. Ribarsky, to be submitted.

6. Y. Takada, J. Phys. Soc. Jpn. <u>45</u>, 786 (1978).

7. N. B. Brandt, S. V. Kuvshinnikov, A. O. Rusakov and V. M. Smernov, JETP Lett. <u>27</u>, 33 (1978).

8. C. W. Chu, A. P. Rusakov, S. Huang, S. Early, T. H. Geballe and C. Y. Huang, Phys. Rev. B <u>18</u>, 2116 (1978).

9. I. Lefkowitz, J. S. Manning and P. E. Bloomfield, Phys. Rev. B <u>20</u>, 4506 (1979).

10. A. B. Kunz and R. S. Weidman, J. Phys. C <u>12</u>, L371 (1979).

11. A. Zunger and M. L. Cohen, Phys. Rev. B <u>20</u>, 1189 (1979).

12. L. Kleinman and K. Mednick, Phys. Rev. B <u>20</u>, 2487 (1979).

13. T. C. Collins, M. Seel and J. J. Ladik, Phys. Rev. B <u>27</u>, 140 (1983).

14. M. Cardona, Phys. Rev. <u>129</u>, 69 (1963).

15. J. C. Slater, <u>Symmetry and Energy Bands in Crystals</u> (Dover, New York, 1972). p. 347.

16. A. J. H. Wachters, J. Chem. Phys. <u>52</u>, 1033 (1970).

17. E. Fiorino and R. Del Sole, Phys. Stat. Sol. B <u>119</u>, 315 (1983).

18. M. W. Ribarsky, W. Luedtke and Uzi Landman, 44th Physical Electronics Conf. (June, 1984).

19. S. Andersson, C. Nyberg and C. G. Tengstal, Chem. Phys. Lett. <u>104</u>, 305 (1984).

20. M. W. Ribarsky, W. Luedtke, and Uzi Landman, submitted to Rapid Communications, Phys. Rev. B.

END

FILMED

11-85

DTIC